High order RBF-FD approximations with application to a scattering problem

Jure Slak
Parallel and Distributed Systems Laboratory,
"Jožef Stefan" Institute,
Jamova cesta 39, 1000 Ljubljana, Slovenia
and
Faculty of Mathematics and Physics,
University of Ljubljana,
Jadranska ulica 19, 1000 Ljubljana, Slovenia
Email: jure.slak@ijs.si

Blaž Stojanovič
Parallel and Distributed Systems Laboratory,
"Jožef Stefan" Institute,
Jamova cesta 39, 1000 Ljubljana, Slovenia
and
Faculty of Mathematics and Physics,
University of Ljubljana,
Jadranska ulica 19, 1000 Ljubljana, Slovenia
Email: blaz.stojanovic@student.fmf.uni-lj.si

Gregor Kosec
Parallel and Distributed Systems Laboratory,
"Jožef Stefan" Institute,
Jamova cesta 39, 1000 Ljubljana, Slovenia
Email: gregor.kosec@ijs.si

***Abstract*—A recently suggested technique for high order meshless approximations is described and analyzed in this paper. It involves constructing ordinary Radial Basis Function-generated finite difference approximations augmented with monomials up to a given order to ensure higher convergence rates. These approximations are used to solve the Poisson's equation on an annulus to demonstrate the predicted convergence rates. The presented methodology is then applied to a scattering problem, which is described by a coupled system of two complex-valued PDEs on two domains, sharing a common boundary.**

***Index Terms*—meshless, RBF-FD, polyharmonic splines, high order approximation, scattering**

I. Introduction

Radial basis function-generated finite differences (RBF-FD) were suggested among others by Tolstykh and Shirobokov [1]. They combine good approximation properties of radial basis functions (RBFs) with their ability to adapt to scattered grids, as the Lagrange interpolation problem can be shown to be nonsingular for many commonly used RBFs [2]. This comes contrary to other suggested generalizations of finite differences to scattered grids, such as the Finite Point method [3], where no such guarantee is given.

Most RBFs, such as the often used Gaussian, multiquadric or inverse multiquadric functions, depend on a so-called shape parameter ϵ, which governs their flatness. This parameter primarily impacts the quality of and the conditioning of the approximation [4]. Extensive research was conducted on selecting the optimal shape parameter [5] and on circumventing the bad conditioning as $\epsilon \to 0$ with specialized algorithms, such as RBF-QR [6].

To avoid these problems altogether, use of polyharmonic splines (PHS) has been suggested, since they do not depend on the shape parameter and do not share the conditioning problems of other RBFs. As PHS themselves do not provide convergent approximations, they mush be augmented with polynomials, and effects of such augmentation have been studied extensively in recent papers [7]–[9].

RBF-FD has since its introduction been widely used in a number of different areas, such as simulation of natural convection around electrical power lines [10], geosciences [11], contact problems [12], option pricing [13] and PDEs on surfaces [14]. Besides those applications, meshless and other mesh-reduction methods have emerged as an attractive alternative to classical methods for a variety of electromagnetic problems [15]–[17]. Specifically, the electromagnetic scattering problem by anisotropic cylinders has been solved using global strong form approaches, such as the method of approximate particular solution (MAPS) [18] and a local weak form approaches, such as the meshfree local Petrov-Galerkin method (MLPG) [19].

The rest of the paper is organized as follows: high order RBF-FD discretizations are described in section II and numerical examples are presented in section III, including the Poisson equation in section III-A and a scattering problem in section III-B. Finally, conclusions are presented in section IV.

The authors would like to acknowledge the financial support of the Research Foundation Flanders (FWO), The Luxembourg National Research Fund (FNR) and Slovenian Research Agency (ARRS) in the framework of the FWO Lead Agency project: G018916N Multi-analysis of fretting fatigue using physical and virtual experiments and the ARRS research core funding No. P2-0095.

II. Method description

A. RBF-FD approximations

The core of strong form meshless discretization procedures is the approximation of partial differential operators. Consider a partial differential operator $\mathcal{L}$ at a point $\boldsymbol{x}^*$. We seek an approximation of $\mathcal{L}$ at $\boldsymbol{x}^*$ as a linear combination of function values in neighboring nodes:

$$(\mathcal{L}u)(\boldsymbol{x}^*) \approx \sum_{i=1}^{n} w_i u(\boldsymbol{x}_i). \tag{1}$$

Here $\boldsymbol{x}_i$ represent the *stencil* or *support* at $\boldsymbol{x}^*$, w_i are called *stencil weights*, n is the *stencil size* and u is an arbitrary function. If the weights and function values are assembled into vectors of length n, the approximation is written simply as

$$(\mathcal{L}u)(\boldsymbol{x}^*) \approx \boldsymbol{w}_{\mathcal{L}}(\boldsymbol{x}^*)^{\mathsf{T}}\boldsymbol{u}, \tag{2}$$

where the dependence of $\boldsymbol{w}$ on $\mathcal{L}$ and $\boldsymbol{x}^*$ has been written explicitly. To determine the weights, equality of (1) is enforced for a given set of functions, often monomials [3]. In the RBF-FD discretization, the equality is enforced for radial basis functions, i.e. functions of form

$$\phi(r), r = \|\boldsymbol{x} - \boldsymbol{x}_i\|, \tag{3}$$

which are radially symmetric and centered at stencil nodes $\boldsymbol{x}_i$. Each RBF corresponds to one linear equation for unknowns w_i by enforcing exactness of (1). Assembling these n equations for into matrix form, we obtain the following linear system:

$$\begin{bmatrix} \phi(\|\boldsymbol{x}_1 - \boldsymbol{x}_1\|) & \cdots & \phi(\|\boldsymbol{x}_n - \boldsymbol{x}_1\|) \\ \vdots & \ddots & \vdots \\ \phi(\|\boldsymbol{x}_1 - \boldsymbol{x}_n\|) & \cdots & \phi(\|\boldsymbol{x}_n - \boldsymbol{x}_n\|) \end{bmatrix} \begin{bmatrix} w_1 \\ \vdots \\ w_n \end{bmatrix} = \begin{bmatrix} \ell_{\phi,1} \\ \vdots \\ \ell_{\phi,n} \end{bmatrix}, \tag{4}$$

$$\ell_{\phi,j} = (\mathcal{L}\phi(\|\boldsymbol{x} - \boldsymbol{x}_j\|))|_{\boldsymbol{x}=\boldsymbol{x}^*}, \tag{5}$$

or, written more compactly,

$$A\boldsymbol{w} = \boldsymbol{\ell}_{\phi}. \tag{6}$$

This system is symmetric, and for some ϕ even positive definite [2]. Weights obtained by solving (4) are not necessarily a good approximation of $\mathcal{L}|_{\boldsymbol{x}^*}$ and can be augmented with monomials to improve accuracy.

Let $p_1, \ldots, p_s$ be polynomials for which exactness of (1) is desired. These are often monomials up to a chosen order m, resulting in $s = \binom{m+2}{m}$ additional monomials in 2 dimensions. These additional constraints are enforced by extending (6) as

$$\begin{bmatrix} A & P \\ P^{\mathsf{T}} & 0 \end{bmatrix} \begin{bmatrix} \boldsymbol{w} \\ \boldsymbol{\lambda} \end{bmatrix} = \begin{bmatrix} \boldsymbol{\ell}_{\phi} \\ \boldsymbol{\ell}_p \end{bmatrix}, \tag{7}$$

where

$$P = \begin{bmatrix} p_1(\boldsymbol{x}_1) & \cdots & p_s(\boldsymbol{x}_1) \\ \vdots & \ddots & \vdots \\ p_1(\boldsymbol{x}_n) & \cdots & p_s(\boldsymbol{x}_n) \end{bmatrix} \tag{8}$$

is a $n \times s$ matrix of polynomials evaluated at stencil nodes and

$$\boldsymbol{\ell}_p = \begin{bmatrix} (\mathcal{L}p_1)|_{\boldsymbol{x}=\boldsymbol{x}^*} \\ \vdots \\ (\mathcal{L}p_s)|_{\boldsymbol{x}=\boldsymbol{x}^*} \end{bmatrix} \tag{9}$$

is the vector of values, given by applying considered operator $\mathcal{L}$ to the polynomials at $\boldsymbol{x}^*$. Weights obtained by solving (7) are taken as approximations of $\mathcal{L}$ at $\boldsymbol{x}^*$. Additional unknowns $\boldsymbol{\lambda}$ play the role of Lagrange multipliers and are discarded.

B. Polyharmonic splines with high order augmentation

Common choices for RBFs include Gaussian,

$$\phi(r) = \exp(-(\epsilon r)^2), \tag{10}$$

or multiquadric,

$$\phi(r) = \sqrt{1 + (\epsilon r)^2}. \tag{11}$$

Both of these, along with many other types of RBFs, depend on a shape parameter ϵ, which represents a trade-off between accuracy and stability. Another class of RBFs are the polyharmonic splines, defined as

$$\phi(r) = r^k, \ k \text{ odd}, \tag{12}$$

which do not depend on a shape parameter and the condition number of matrix A (6) remains constant under refinement. PHS should be augmented with monomials of at least second order to obtain convergent results, but can be augmented with much higher orders to achieve higher convergence rates and orders of accuracy.

C. PDE discretization

Consider a boundary value problem

$$\begin{aligned} \mathcal{L}u &= f \text{ in } \Omega, \\ u &= g \text{ on } \partial\Omega. \end{aligned} \tag{13}$$

Domain Ω is discretize by placing N nodes in the domain, N_i in the interior and N_b on the boundary. Then, stencils $N_{\boldsymbol{x}_i}$ are selected for each node $\boldsymbol{x}_i$, usually by taking n closest nodes. For PHS RBFs augmented with s monomials it has been recommended taking at least $n = 2s$ nodes [8]. Each operator $\mathcal{L}$ is approximated at every point where it needs to be evaluated using the procedure described in section II-A. For problem (13) we would approximate $\mathcal{L}$ at all interior nodes.

This approximation replaces the equation $(\mathcal{L}u)(x_i) = f(x_i)$ with a linear equation

$$\boldsymbol{w}_{\mathcal{L}}(\boldsymbol{x}_i)^{\mathsf{T}}\boldsymbol{u} = \boldsymbol{f}, \tag{14}$$

where vectors $\boldsymbol{u}$ and $\boldsymbol{f}$ represent values of functions f and u in stencil nodes of $\boldsymbol{x}_i$. The N_i equations (14) can be assembled into a system of equations, along with N_b equations for boundary conditions, to obtain a $N \times N$ sparse linear system with approximately Nn nonzero elements. The solution of this system is a numerical approximation of u and its values are known only at nodes x_i and are denoted u_i.

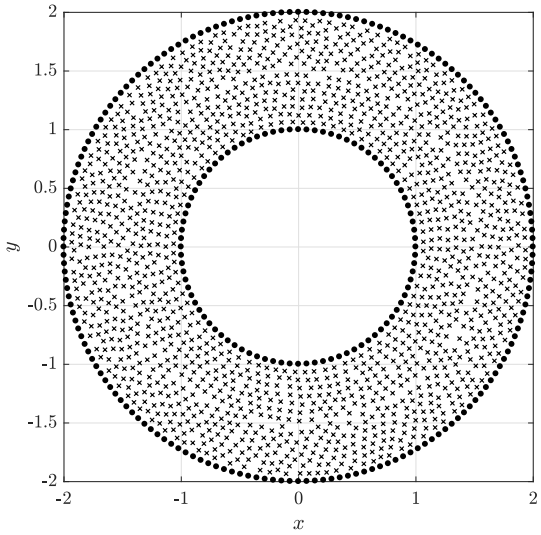

Fig. 1. One of the scattered node distributions when solving (15), showing boundary and internal nodes. The total number of nodes is $N = 1709$.

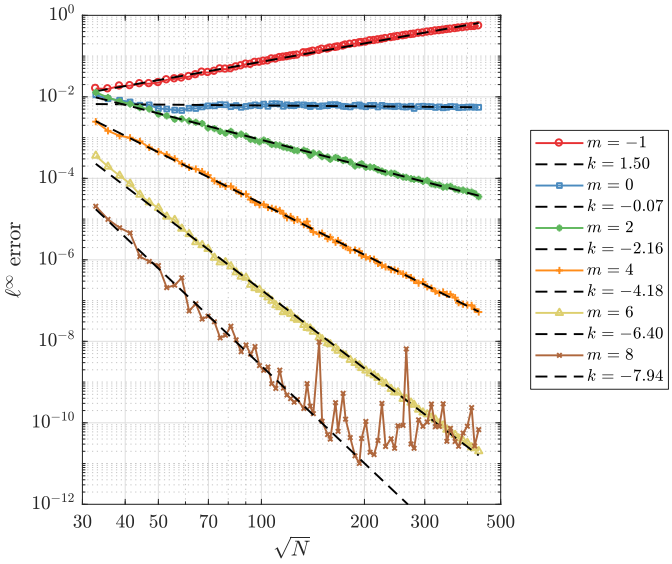

Fig. 2. Convergence of the RBF-FD method using PHS with various orders of monomial augmentation. Values of k represent line slopes for the preceding data series. Measuring in other error norms, such as ℓ^1 or ℓ^2 gave similar results.

III. Numerical examples

A. Poisson equation

First we consider Poisson's equation

$$\begin{aligned} \nabla^2 u &= f \text{ in } \Omega, \\ u &= g \text{ on } \partial\Omega \end{aligned} \tag{15}$$

on an annulus domain, centered at the origin with radii r_1 and r_2, i.e.

$$\Omega = \{(x, y);\ r_1^2 < x^2 + y^2 < r_2^2\}. \tag{16}$$

We choose $u(x, y) = \sin(\pi x)\sin(\pi y)$ as the test function and compute f and g accordingly. Additionally, we choose $r_1 = 1$ and $r_2 = 2$.

Problem, given by (15), was solved using RBF-FD with polyharmonic splines as basis functions. The function were augmented with monomials up to order m, with $m = -1$ representing no monomial augmentation. The nodes were placed in the domain using a node positioning algorithm suitable for mesh-free discretizations [20], which results in scattered node distributions, as shown in Fig. 1. The number of nodes varied from 1000 to 180 000 and the stencil for each node was comprised of $n = 65$ closest nodes. The error was measured in relative discrete infinity norm as

$$\ell_\infty = \frac{\max_i |u(\boldsymbol{x}_i) - u_i|}{\max_i |u(\boldsymbol{x}_i)|}. \tag{17}$$

The measured errors for various m with respect to N are shown in Fig. 2.

If can be seen that PHS approximations diverge, if computed without augmentation or augmented only with a constant. For augmentation of higher order, convergence rates correspond to the order of the added monomials. The convergence is also surprisingly smooth for a meshless method on scattered node sets. The method at $m = 8$ loses a bit of its robustness, partially due to high order of monomials, but also due to the number of monomials $s = \binom{8+2}{2} = 45$ being relatively large compared to the stencil size $n = 65$. The stagnation of error for $\sqrt{N} \geq 200$ in $m = 8$ case is due to finite precision arithmetic.

B. Scattering problem

Consider an infinitely long anisotropic dielectric cylindrical scatterer surrounded by free space and let $D \subset \mathbb{R}^2$ be its cross section, with an outward normal $\vec{n}$ on boundary ∂D. A 2×2 symmetric positive definite matrix of relative magnetic permeabilities A_μ is used to describe the anisotropy.

The scatterer is excited by an $e^{i\omega t}$ time-harmonic plane wave with $\mathbf{TM}^z$ polarization, with ω standing for its angular frequency. Let v denote the complex-valued field inside the scatterer and u the field outside of the scatterer. Field u can be further decomposed into the known incident u^i and the unknown scattered field u^s. The scattering of u^i can be described as a system of complex PDEs for v and u^s:

$$\nabla \cdot A_\mu \nabla v + \epsilon_r k^2 v = 0 \quad \text{in} \quad D, \tag{18}$$

$$\nabla^2 u^s + k^2 u^s = 0 \quad \text{in} \quad \mathbb{R}^2 \setminus D, \tag{19}$$

with boundary conditions

$$v - u^s = u^i \quad \text{on} \quad \partial D \tag{20}$$

$$\frac{\partial v}{\partial \vec{n}_{A_\mu}} - \frac{\partial u^s}{\partial \vec{n}} = \frac{\partial u^i}{\partial \vec{n}} \quad \text{on} \quad \partial D, \tag{21}$$

$$\lim_{r \to \infty} \sqrt{r} \left(\frac{\partial u^s}{\partial r} - iku^s \right) = 0, \tag{22}$$

where $k = \omega\sqrt{\mu_0 \epsilon_0} = \frac{2\pi}{\lambda}$ is the wave number of free space, μ_0 and ϵ_0 are magnetic permeability and electric permittivity of free space, and ϵ_r is the relative electric permittivity of the

scatterer. Relative magnetic permeability matrix A_μ is written as

$$A_\mu = \frac{1}{\mu_{xx}\mu_{yy} - \mu_{xy}^2} \begin{bmatrix} \mu_{xx} & \mu_{xy} \\ \mu_{xy} & \mu_{yy} \end{bmatrix} \tag{23}$$

and the anisotropic normal derivative is defined as

$$\frac{\partial v}{\partial \vec{n}_{A_\mu}} = \vec{n} \cdot A_\mu \nabla v. \tag{24}$$

The condition (22) is the so called Sommerfield boundary condition.

To solve the described problem numerically, a finite annulus Ω is constructed around D, as seen in Figure 3. This bounds the free space $\mathbb{R}^2$ by outer boundary of Ω, which implies (19) is now only solved in Ω and the outer boundary condition (22) changes to:

$$\frac{\partial u^s}{\partial \vec{n}} + \left(ik + \frac{1}{2r_2} \right) u^s = 0 \quad \text{on} \quad \partial\Omega. \tag{25}$$

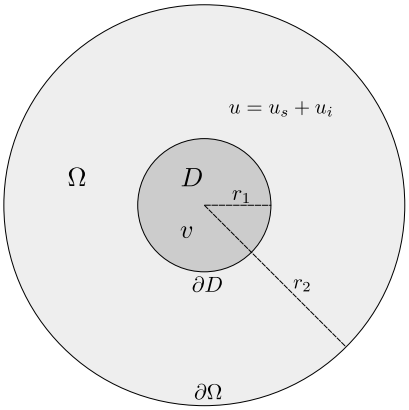

Fig. 3. Computational domain Ω with a cylindrical scatterer cross-section in the middle.

The numerical problem is a coupled system of complex-valued PDEs on two domains Ω and D with a common boundary ∂D. The RBF-FD method with PHS, augmented with monomials up to order $m = 4$, is used to obtain the discrete formulation. Each of the domains Ω and D is discretized separately. The total number of nodes used was $N_D = 10\,872$ for discretization of D and $N_\Omega = 86\,116$ for discretization of Ω. Certain care needs to be taken when constructing the discretization along the boundary of D, as we need to make sure that the nodes correspond exactly with the nodes on the interior boundary of Ω. When constructing the final $(N_\Omega + N_D) \times (N_\Omega + N_D)$ matrix, the equations (18), (19) and (25) are enforced as usual. The conditions (20) and (21) are the ones that couple the fields together and must be enforced so that the nodes on the boundary of D are used when discretizing v and the corresponding nodes on the boundary of Ω are used when discretizing u^s.

Values $r_1 = 0.25$, $r_2 = 0.75$, $\epsilon_r = 0.5$, $\mu_{xx} = 2$, $\mu_{xy} = 0.5$, $\mu_{yy} = 1$ were used for the undetermined physical constants.

The computed field v inside the scatterer is shown in Fig. 4 and field u^s is shown in Fig. 4. The error evaluated against an analytical solution [21] is of order 10^{-2} for both computed fields.

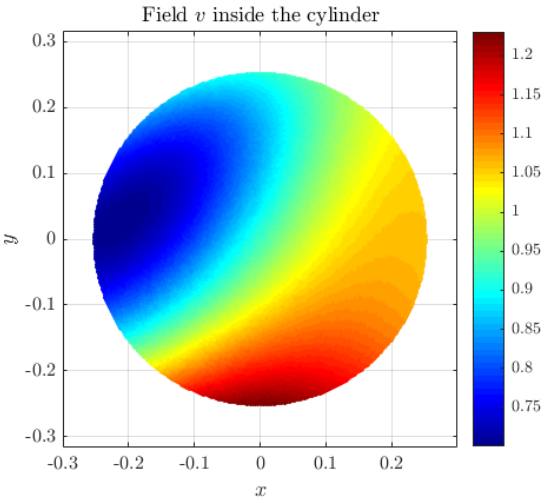

Fig. 4. Magnitude of v inside the scatterer.

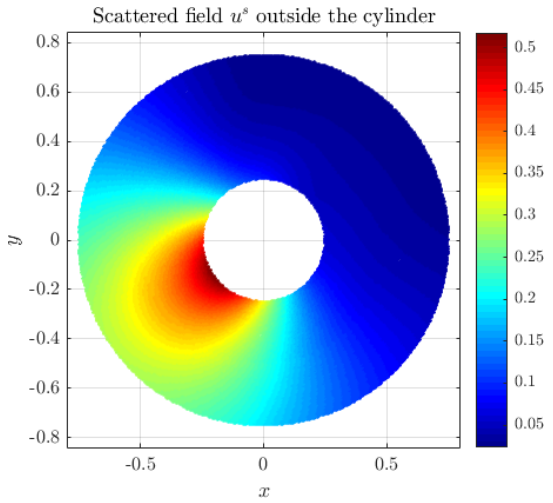

Fig. 5. Magnitude of u^s around the scatterer.

IV. Conclusions

We have presented a RBF-FD discretization technique using polyharmonic splines with polynomial augmentation. It was shown that up to 8th order convergence can be achieved on scattered node sets relatively simply by augmenting with monomials of appropriate order and taking large enough stencils. This technique was applied to solve a scattering problem, which involved solving a coupled system of two complex-valued PDEs on two domains, sharing a common boundary.

All computations were performed using the in house Medusa library [22] for meshless PDE discretizations. Future work will focus on developing adaptive techniques and error indicators for RBF-FD, to aid in solving real world engineering problems.

REFERENCES

[1] A. Tolstykh and D. Shirobokov, "On using radial basis functions in a "finite difference mode" with applications to elasticity problems," *Computational Mechanics*, vol. 33, no. 1, pp. 68–79, 2003.

[2] M. D. Buhmann, *Radial basis functions: theory and implementations*. Cambridge university press, 2003, vol. 12.

[3] E. Oñate, F. Perazzo, and J. Miquel, "A finite point method for elasticity problems," *Computers & Structures*, vol. 79, no. 22-25, pp. 2151–2163, 2001.

[4] R. Schaback, "Error estimates and condition numbers for radial basis function interpolation," *Advances in Computational Mathematics*, vol. 3, no. 3, pp. 251–264, 1995.

[5] G. E. Fasshauer and J. G. Zhang, "On choosing "optimal" shape parameters for RBF approximation," *Numerical Algorithms*, vol. 45, no. 1-4, pp. 345–368, 2007.

[6] B. Fornberg, E. Lehto, and C. Powell, "Stable calculation of Gaussian-based RBF-FD stencils," *Computers & Mathematics with Applications*, vol. 65, no. 4, pp. 627–637, 2013.

[7] N. Flyer, B. Fornberg, V. Bayona, and G. A. Barnett, "On the role of polynomials in RBF-FD approximations: I. Interpolation and accuracy," *Journal of Computational Physics*, vol. 321, pp. 21–38, 2016.

[8] V. Bayona, N. Flyer, B. Fornberg, and G. A. Barnett, "On the role of polynomials in RBF-FD approximations: II. Numerical solution of elliptic PDEs," *Journal of Computational Physics*, vol. 332, pp. 257–273, 2017.

[9] V. Bayona, N. Flyer, and B. Fornberg, "On the role of polynomials in RBF-FD approximations: III. Behavior near domain boundaries," *Journal of Computational Physics*, vol. 380, pp. 378–399, 2019.

[10] G. Kosec and J. Slak, "RBF-FD based dynamic thermal rating of overhead power lines," in *Advances in fluid mechanics XII*, ser. WIT transactions on engineering sciences, S. Hernández, L. Škerget, and J. Ravnik, Eds., vol. 120, Wessex institute. WIT press, 2018, pp. 255–262.

[11] B. Fornberg and N. Flyer, *A primer on radial basis functions with applications to the geosciences*. SIAM, 2015.

[12] J. Slak and G. Kosec, "Adaptive RBF-FD method for contact problems," *preprint, arXiv:1811.10368 [math.NA]*, 2018. [Online]. Available: https://arxiv.org/abs/1811.10368

[13] N. Thakoor, D. Y. Tangman, and M. Bhuruth, "RBF-FD schemes for option valuation under models with price-dependent and stochastic volatility," *Engineering Analysis with Boundary Elements*, vol. 92, pp. 207–217, 2018.

[14] A. Petras, L. Ling, and S. J. Ruuth, "An RBF-FD closest point method for solving PDEs on surfaces," *Journal of Computational Physics*, vol. 370, pp. 43–57, 2018.

[15] Y. Marchal, "Some meshless methods for electromagnetic field computation," *IEEE Trans. Magn.*, vol. 34, no. 5, pp. 3351–3354, 1998.

[16] S. L. Ho, S. Yang, J. M. Machado, and H. C. Wong, "Application of a meshless method in electromagnetics," *IEEE Transactions on Magnetics*, vol. 37, no. 5, pp. 3198–3202, 2001.

[17] D. Poljak, M. Cvetković, D. Cavka, A. Peratta, C. Peratta, H. Dodig, and A. Hirata, "Boundary integral methods in bioelectromagnetics and biomedical applications of electromagnetic fields," in *Boundary Elements and other Mesh Reduction Methods XXXXI*. WIT Press, sep 2018.

[18] M. H. Esfahani, H. R. Ghehsareh, and S. K. Etesami, "The extended method of approximate particular solutions to simulate two-dimensional electromagnetic scattering from arbitrary shaped anisotropic objects," *Engineering Analysis with Boundary Elements*, vol. 82, pp. 91–97, 2017.

[19] ——, "A meshless method for the investigation of electromagnetic scattering from arbitrary shaped anisotropic cylindrical objects," *Journal of Electromagnetic Waves and Applications*, vol. 31, no. 5, pp. 477–494, 2017.

[20] J. Slak and G. Kosec, "On generation of node distributions for meshless PDE discretizations," *arXiv:1812.03160 [math.NA]*, 2018, preprint, available at https://arxiv.org/abs/1812.03160.

[21] J. C. Monzon and N. Damaskos, "Two-dimensional scattering by a homogeneous anisotropic rod," *IEEE Transactions on Antennas and Propagation*, vol. 34, no. 10, pp. 1243–1249, 1986.

[22] J. Slak and G. Kosec, "Parallel coordinate free implementation of local meshless method," in *2018 41st International Convention on Information and Communication Technology, Electronics and Microelectronics (MIPRO)*. IEEE, 2018, pp. 0172–0178, http://e6.ijs.si/medusa.